Heliyon 7 (2021) e08294

Contents lists available at ScienceDirect

Heliyon

journal homepage: www.cell.com/heliyon

Research article

Hydroxypropylmethyl cellulose (HPMC) crosslinked keratin/hydroxyapatite (HA) scaffold fabrication, characterization and *in vitro* biocompatibility assessment as a bone graft for alveolar bone regeneration

Sandleen Feroz *, George Dias

Department of Anatomy, School of Biomedical Sciences, University of Otago, Dunedin, 9054, New Zealand

ARTICLE INFO

Keywords:
Keratin
(Hydroxypropyl) methylcellulose
Hydroxyapatite
Alveolar bone
Dental implants
Tissue engineering

ABSTRACT

Wool derived keratin has garnered significant advancements in the field of biomaterials for hard tissue regeneration. The main limitation of keratin-based biomaterials for bone tissue engineering is their fragile nature. This paper proposes the development of a novel hydroxypropyl methylcellulose (HPMC) crosslinked keratin scaffold, containing hydroxyapatite as a major inorganic component by freeze drying technique for alveolar bone regeneration. The prepared keratin/hydroxyapatite/HPMC (K/HA/HPMC) scaffold was characterized to study its chemical, physical, and mechanical properties by Scanning electron microscope (SEM), Fourier transform infrared spectroscopy (FTIR), Energy dispersive X-ray spectroscopy (EDX), X-Ray diffractometric (XRD) analysis. The SEM images of the scaffolds showed highly porous interconnected architecture with average pore size of 108.36 ± 22.56 while microcomputed tomographic analysis measured total porosity as 79.65 %±. Energy dispersive X-ray spectroscopic (EDX) analysis confirmed that inorganic component of scaffold was mainly composed of calcium and phosphorous ions having Ca/P molar ration of 1.6. The maximum compressive strength was found to be in the range of 0.841 ± 0.37 MPa. Furthermore, the K/HA/HPMC scaffold was structurally stable and weight loss of about 26% was observed when soaked in phosphate buffered solution (PBS) for 28 days. In vitro biocompatibility testing showed that K/HA/HPMC scaffold was cytocompatible and supported the attachment, proliferation of osteoblast (Saos-2) cells. Thus, the development of a non-toxic chemical cross-linking system with HPMC was investigated to fabricate K/HA/HPMC scaffold and our results showed great potential of these scaffolds to regenerate alveolar bone due to their structural similarity and excellent in vitro biocompatibility.

1. Introduction

Alveolar bone which provides support to dentition is a dynamic structure undergoing continuous remodelling according to functional needs. There are numbers of local and systemic factors which results in progressive loss of this functional bone [1]. Most common clinical problem after tooth loss is the resorption of alveolar bone, especially in the anterior aesthetically important region. The application of dental implants to restore the lost teeth has now emerged as a very popular treatment modality due to overall procedure predictability, low failure rate, as well as its durability [2, 3, 4]. For the successful placement of titatnium screw implants, specific dimensions of alveolar ridge is crucial to allow greater available surface area for osseointegration [5]. Clinically the placement of short or narrow dental implants in resorbed alveolar bone regions is commonly practised, to achieve desirable prosthetic results. However, research in implant dentistry has reported lower success rates due to reduced implant to bone contact surface area to provide required anchorage and stability [6, 7] Thus, the role of tissue engineers becomes very important to developed materials or techniques to promote bone regeneration with predictable outcomes.

Bone grafting is extensively used in the field of orthopaedics to treat and reconstruct the bony defects. Currently, allografts and autografts are the most commonly used bone grafting procedure, but these often present some major drawbacks such as immunogenic reactions, morbidity of donor site, poor quality of donor bone due to underlying bone diseases etc. Thus, due to all these procedure related complexities, there is dire demand at both scientific and commercial level to develop more efficient treatment options that surpass the need of these allografts/autografts for bone regeneration. In last few decades, the field of tissue engineering has offered many advancements at nano level for hard tissue regeneration [8,

* Corresponding author.
E-mail address: fersa942@student.otago.ac.nz (S. Feroz).

https://doi.org/10.1016/j.heliyon.2021.e08294
Received 11 July 2021; Received in revised form 8 September 2021; Accepted 27 October 2021

9, 10, 11]. Recently, fabrication of three dimensional, biocompatible, biodegradable scaffolds for bone regeneration has opened new perspective for research in this field. Freeze drying, 3-D printing, SBF immersion technique, cryogelation method, electrospinning are some of the extensively used procedures in the preparation of artificial hybrid matrices for treatment of damaged or diseased bony defects [12, 13, 14, 15, 16]. In our current study we report the preparation of K/HA/HPMC porous composite scaffold by using freeze drying technique. This technique also known as lyophilization, or ice templating has been demonstrated as a promising method for various tissue engineering applications [17, 18, 19]. With this technology 3-dimmensional scaffolds could be designed having more than 90% porosity and pore diameter in the range of 20–400μm [19, 20]. The porosity and shape of scaffolds can be managed by altering certain factors of the process, such as solution and instrumental parameters, which results in improved biological and mechanical properties of the scaffolds [20]. This process is studied on wide range of materials such as ceramics, organic – soluble polymer and water-soluble polymer [21, 22, 23, 24]. Freeze drying offers several advantages over other commonly used methods. Unlike electrospinning, water is used as solvent instead of toxic chemicals which makes overall process green and environment friendly as there are no chances of toxicity due to chemical residues in the prepared scaffolds [21, 25]. Furthermore, this method can be combined with other techniques such as gel casting, salt leaching, liquid dispensing for improved final properties of scaffolds [26, 27, 28, 29]. Thus, some of the practical limitations associated with conventional electrospinning technique such as insufficient mechanical strength for application in load bearing areas, possible toxicity of cross linkers or solvents, poor cellular infiltration can be overcome by freeze drying technology [25, 30, 31]. Another advantage associated with freeze drying is safe processing of heat sensitive drugs, growth factors or proteins as no heat is involved during the process.

During the past few years, there has been extensive research on keratin at both macro and nano scale as a potential material for various biomedical applications [8]. The distinct properties of this natural polymer such as intrinsic biological activity, mechanical durability, good biocompatibility results in the wide application of keratin in the field of modern regenerative medicine [32, 33]. Hair, wool, nails, feathers are some of the rich sources of this autogenous protein [8]. Natural bone is a composite structure mainly composed of inorganic biomineral (hydroxyapatite) which comprises of 60–70 % of bone, therefore, application of pure synthetic hydroxyapatite as a bone graft substitutes has been investigated extensively in number of in *vitro* and in *vivo* studies [34, 35, 36]. It was observed that it has osteogenic potential without causing any inflammatory response or toxicity. However, due to its brittle nature and poor strength these pure hydroxyapatite are not ideal substituted material for bone regeneration in load bearing areas [10]. To closely emulate the architecture of natural bone many researchers proposed different strategies to design porous scaffolds based on polymers and hydroxyapatite [32, 37]. Levingstone et al. designed a layered composite to closely mimic the bone density which gradually increases from inside out. However, this layered scaffold failed to achieve biomimetic function fully [37]. In the past, mixing of hydroxyapatite and keratin has proven to be a successful approach towards designing hybrid biomaterials having improved mechanical strength, excellent biocompatibility and desirable porosity [18, 38, 39]. Tachibana et al. proposed the immersion of keratin sponges in buffer solution containing calcium and phosphate ions. Though these composite sponges exhibited initial nucleation sites of the calcium phosphate, but scaffolds prepared by this technique lacked the continuous interconnected porous structure along with poor mechanical strength [39]. Our group previously worked on two techniques to produce porous keratin/HA scaffolds. These methods mainly involve mixing of ice microparticles to keratin/HA aqueous suspension and compression moulding. The results of in vivo implantation in animals showed good biocompatibility of these scaffolds. However, high density of these keratin/HA composite sponges and complex fabrication technique might limit their wide application in bone tissue engineering [38, 40].

Recently, cross-linking emerged as a promising strategy to design novel tissue engineered scaffolds with improved biomechanical properties specific to their application [41]. A cross-linking agent forms a chemical or physical bond to connect the polymeric chain functional groups through supramolecular bonding or covalent interactions [42]. Previously various cross-linking techniques have been utilized by researchers to modify the mechanical, biological and degradation properties of the fabricated scaffolds such as chemical crosslinking by glutaraldehyde or physical crosslinking by using dry heating treatment (DHT) etc [8, 43, 44]. Kim et al. cross-linked keratin/chitosan scaffolds with glutaraldehyde to prepare skin grafts [45]. Similarly, Li Chen et al. designed biomimetic porous collagen/HA scaffold for bone tissue engineering using glutaraldehyde as a cross-linking agent [17]. However, the presence of free aldehyde groups, when glutaraldehyde used as a cross-linker can cause cell toxicity and inflammatory reactions in the body. The glutaraldehyde cross-linked scaffolds require additional washing with amino acid or free amine groups solution to remove free aldehyde groups and to improve their biocompatibility [46]. . Therefore, there is a dire demand for exploring new technologies involving nontoxic, green chemicals for crosslinking of natural polymers.

Our current project is a part of an ongoing effort to design a composite scaffold closely mimicking the porous architecture of trabecular part of human alveolar bone using green, non-toxic cross linker to further improve the degradation, mechanical and biological properties of the scaffold. In this project, keratin was extracted using a patented technique and hydroxypropyl methyl cellulose (HPMC) was used as a cross-linking agent [47]. HPMC crosslinked, highly porous keratin scaffolds containing nanocrystalline hydroxyapatite as major inorganic component were fabricated by using a freeze-drying technique. HPMC is a hydrophilic, biodegradable polymer which is approved by United States Food and Drug Administration (FDA) for use in controlled release formulations [48]. The presence of HPMC provides additional sites of interaction for keratin and hydroxyapatite particles and thus aid in the formation of highly porous anisotropic structure. Previously, several studies showed the application of HPMC as a plasticizing agent to fill bone defects or to improve the mechanical properties of bone cements [49, 50, 51]. Ather et al. reported the preparation and characterization of highly porous chitosan/HA scaffolds using HPMC as a gelation agent [52]. Furthermore, another study reported the preparation of HPMC cross-linked chitosan scaffolds as a potential matrices for regeneration of alveolar bone [48]. As per our knowledge there is no study conducted so far to explore the application of HPMC as cross-linking agent for developing keratin derived scaffolds for bone regeneration. Therefore, the aim of our current investigation is to design interconnected, porous keratin/hydroxyapatite scaffolds utilising HPMC as a cross linker. After fabrication, the structure of the scaffold was investigated with using Scanning electron microscopy followed by Fourier transform infrared spectroscopy (FTIR), microcomputed tomography (u-CT) imaging, energy dispersive X-ray spectroscopy (EDX) and X-ray diffractometer (XRD). The degradation behaviour and in vitro biological activity of the scaffold was also investigated. The biocompatibility of the construct was studied by using human Saos-2 cell lines by cell viability and cell proliferation assays.

2. Materials and methods

2.1. Materials

Hydroxyapatite powder was purchased from Sigma-Aldrich, St. Louis, USA. Streptomycin, penicillin, trypsin (Gibco, Thermo Fisher scientific). Other chemicals including Bovine serum albumin, acetic acid (glacial, > 99.7%), phosphate buffered saline (PBS) tablets, MTS were purchased from Sigma Aldrich. All the chemicals were used as received without any further purification.

2.2. Extraction of keratin from wool

Keratin powder was extracted from sheep wool using our patented technique [47]. Briefly, 1 gm of wool fibres were added to 20ml mixture containing ascorbic acid (6Mm) and citric acid (90mM). The pH of reaction mixture containing wool fibres was 3.5. For keratin degradation this reaction mixture was expose to electromagnetic energy source from microwaves (Microwave NZ Ltd. Auckland. New Zealand) The process resulted in the generation of three discrete fractions named supernatant, precipitate, and plug. Later studies done on these three fractions showed that supernatant contains high concentration of citric acid (~31% by HPLC). In our current experiments the two amino acid rich fractions i-e, plug and precipitate fractions of wool derived protein were subjected to three washing cycles to eliminate any traces of chemicals followed by freeze drying, grinding, and storing in vacuum -sealed container for future use.

2.3. Synthesis of HPMC crosslinked keratin/hydroxyapatite composite scaffolds

Scaffolds were fabricated by adding keratin powder to water at a concentration of 100 mg/ml under continuous mechanical stirring for 4 h at room temperature. HPMC (250 mg) was added to the keratin mixture followed by continuous stirring for another 4 h 400mg of nano hydroxyapatite powder was added into separate beaker containing small quantity of water, and after ultrasonication at an amplitude of 30 % for about 20 min, then added to the mixture containing keratin/HPMC. This mixture was stirred overnight to achieve complete homogenization. The samples were placed in -80 ^{o}C freezer for about 48 h followed by freeze drying at -50 ^{o}C for 18 h to prepare 3- dimensional K/HA scaffolds crosslinked by HPMC. These scaffolds were stored at room temperature under sterile conditions till further characterization. The pure keratin scaffolds were prepared as a control using freeze-drying technique.

3. Characterization

In the following *in-vitro* study, the prepared scaffolds were characterized to determine their chemical, physical, and biological properties.

3.1. Physio chemical analysis of keratin/HA/HPMC scaffolds

3.1.1. Fourier transform infrared spectroscopy (FTIR)

Fourier transform infrared spectroscopy was used as primary spectroscopic technique to determine the functional groups within a material and interaction at molecular level between different components of scaffolds. Sample preparation for analysis includes grinding of 1mg of sample with 100mg of KBr to prepare a pellet with a pellet press. The analysis was performed by using a Perkin Fourier Transform Infrared Spectrophotometer (Perkin Elmer, 2000 series) at a resolution of 4cm-1 from an average of 32 scans between 4000-400 cm-1.

3.1.2. Energy dispersive X-ray spectroscopy (EDX)

To identify the elemental composition of tested scaffolds energy dispersive X-ray analyser (Oxford UK) operating at 15 mA and 15 kV was used. To determine the elemental composition of each sample four square fields were chosen randomly.

3.1.3. X-ray diffraction (XRD)

The crystallinity of the powder HA, Keratin powder and porous scaffolds were studied by X-ray diffractometer (PANalytical X^{1} Pert PRO MPD System) using Cu-K$^{\alpha}$ radiation source. The scans were recorded in the regions 10°≤2Θ≤70° with step time of 1 s and step size of 0.02°.

3.1.4. Scanning electron microscopy (SEM)

Scanning electron microscope (JOEL 2300, Tokyo Japan) equipped with an Energy dispersive X-ray analyzer (Oxford UK) was used to analyse the microstructure of the scaffolds. All samples were gold coated (80 A°) and studied under SEM at an accelerating voltage of 20 kV.

3.1.5. Microcomputed tomography (μ CT)

Porosity of the keratin/HA/HPMC scaffolds were measured with micro-CT. A 4 mm sample was mounted on Sky Scan 1172 high resolution u CT scanner (Bruker, Kontich, Belgium) holder with modelling clay. The scanner was operated at 30kV voltage and a current of 175 u A respectively. The 2-D images were taken at pixel size of 11.4 um by rotating the sample with 0.4° of rotation per section. The transverse section of the scaffold was imaged 1000 times and all 2-D images were further analyzed by using the CT software (Skyscan, Kontich, Belgium).

3.2. Mechanical characterization

The compressive strength of the pure keratin and K/HA/HPMC scaffolds was measured by using a universal testing machine (INSTRON 3369). The testing was carried out on samples having thickness 5mm and diameter of 10 mm. The compression measurements were observed at a 0.5 mm/min crosshead speed downwards at 25 °C.

3.3. Degradation and structural stability

The *in-vitro* degradation and structural stability of the prepared scaffolds were assessed in phosphate buffered saline (PBS). The pH of PBS (0.01M) was 7.4 prior to scaffolds submersion. All samples were soaked in 10 ml of PBS at 37 °C in an incubator for 3, 7, 14, 21 and 28 days. Initially, the dry weight of all equally weighted samples was measured as W°. After every interval, the samples were withdrawn from PBS, rinsed with deionized water, dried in vacuum dryer for 48 h and weighed (Wt). The degradation of the scaffolds was calculated by measuring the weight loss of each sample according to the following Eq. (1):

$$\text{Mass loss (Wf)} = \frac{W^{\circ} - Wt}{W^{\circ}} \times 100\% \quad (1)$$

W° and Wt denote the weights before and after immersion in PBS. Wf is the rate of weight loss over predetermined time periods.

3.4. Biological properties

3.4.1. Cell viability testing

The prepared K/HA/HPMC scaffolds were tested for in vitro biocompatibility assessment in terms of cytotoxicity, adhesion and proliferation by using human Saos-2 osteoblast -like cells. Pure keratin scaffolds were used as a control. Cells were cultured in minimum essential media alpha (MEM-a) supplemented with 10% foetal bovine serum (FBS) and 1% antibiotics. Cells were grown in culture flasks at 37 °C with 5% CO_2 in an incubator. Cells of 6th passage were used to perform all biological studies. Scaffolds were sterilized by immersing in 70% ethanol (30 min) followed by UV light exposure for 30 min, rinsed gently with PBS and placed in culture media in 48 well plates overnight in a humidified atmosphere at 37° before seeding cells. Culture media was replenished every day, and the cells were seeded at a density of 6×10^{3} cells per scaffold for LIVE/DEAD cytotoxicity and cell proliferation testing. All experiments were performed in triplicates.

After 24, 48 and 72 h, cell viability was assessed with LIVE/DEAD cytotoxicity kit (mammalian cells). Confocal laser scanning microscope (Carl Zeiss Micro Imaging GmbH, Jena, Germany) was used for fluorescent visualisation of the stained cell-scaffold constructs.

All images were captured using Zen 2009 software (Carl Zeiss). Three random fields per scaffold were selected for cell counting by using 10x objective lens and cell viability was measured by following Eq. (2).

$$Cell\ Viability\ (\%) = \frac{Number\ of\ Live\ cells}{Total\ cell\ number} \times 100 \quad (2)$$

3.4.2. Cell proliferation assay

The cell proliferation of Saos-2 cells seeded on keratin and K/HA/HPMC was studied using the MTS [3-(4,5-dimethylthiazol-2yl)-5-(3-caebozymethoxyphenyl)-2-(4,5-dimesulphonyl) _2 H-tetrazolium] assay. This is a calorimetric technique used to determine the reduction of tetrazolium dye to *formazen* by reacting with living cells. After period of 24, 48, 72 h, cell proliferation was observed by calorimetric measurement of absorbance at the wavelength of 490nm using a spectrophotometer (Labtech LT 4500 microplate reader).

3.4.3. Cell adhesion and morphology

The morphology and attachment of Saos-2 cells, grown on the K/HA/HPMC scaffolds were evaluated using SEM imaging technique after 24, 48 and 72 h. Briefly, 6th passage cells were trypsinized and gently seeded on the scaffolds in concentration of 1 × 10^5 cells in 48 well cell culture plates. Scaffolds were incubated in a humidified incubator at 37 °C, 5% CO_2 for 90 min, followed by addition of complete α-MEM media. Keratin/HA/HPMC scaffolds with cells were washed with PBS and fixed with glutaraldehyde (2.5%) in cacodylate buffer (0.1M) at pH of 7.4. All samples were dehydrated by using 30%, 50%, 70%,90% and 100 % ethanol. After gold palladium coating, the SEM images were taken at 15kv voltage at 24, 48 and 72 h of incubation time-points.

4. Statistical analysis

All experimental data was analysed using Prism (GraphPad Prism 6, USA) software. Non-linear curves were reported by their equation and coefficient of determination value (r2). Bar graphs represented as ± standard error of mean. The differences in the mean values between the groups were analyzed by using ANOVA. Tukey's multiple comparison tests were performed to reveal the differences among tested groups at a confidence level of 95% ($P < 0.05$).

5. Results and discussion

5.1. Chemical characterization

5.1.1. FTIR analysis

FT-IR spectra of nano-hydroxyapatite powder, pure keratin powder, HPMC and keratin/HA/HPMC crosslinked composite scaffolds are shown in Figure 1.

Figure 1(A) shows spectrum for pure keratin powder. The characteristic absorption bands of the peptide bonds (–CONH–) were observed. The absorption band at 3276 cm-^{1} corresponds to N–H bond vibrations.

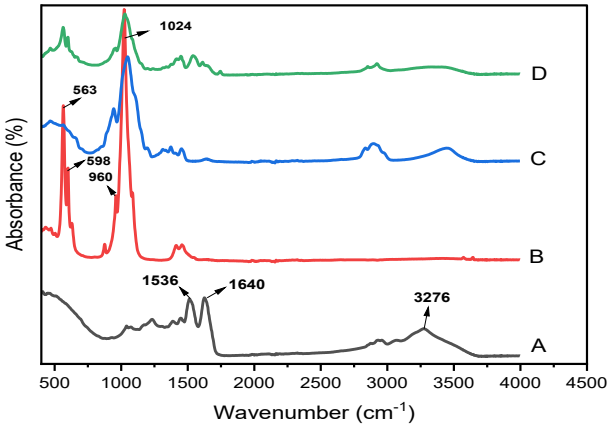

Figure 1. Comparative FTIR spectra of: A) Keratin B) Hydroxyapatite powder C) HPMC powder D) Keratin/HA/HPMC scaffolds.

The sharp peak due to C=O stretching was recorded at 1640 cm-^{1} is related to amide I band. Amide I band vibration frequency was sensitive to protein secondary structure [53]. Another peak observed at 1536cm-^{1} was related to Amide II and it was due to N–H bending and C–H stretching vibrations [54]. Figure 1(B) shows the FT-IR recorded for hydroxyapatite powder. The peaks observed at 1024, 960 belongs to characteristics peaks associated with phosphate group (PO_4). The peaks observed at 598cm-^{1} and 563cm-^{1} were all assigned to P–O stretching coupled with P–O band.

The characteristic vibration peaks associated with HPMC are shown in Figure 1(C). The peaks related to methoxy (-OCH_3) group and pyranose ring appeared at 1496cm-^{1} and 900-950 cm-^{1}.

This pyranose ring vibrations could be seen at 1586cm^1 in FTIR spectrum of K/HA/HPMC scaffold. However, the peak observed for methoxy group was less prominent due to relatively lower concentration of HPMC in the composite scaffolds as shown in Figure 1(D). The characteristic absorption peaks of keratin related to amides I and II were observed at 1631, 1539 cm-^{1} for keratin/HA/HPMC composite scaffolds. A sharp peak for phosphate groups occurred at 1024cm-^{1}.

Thus, FT-IR analysis confirmed the interfacial crosslinking between organic and inorganic component of scaffold. It also indicated the presence of protein secondary structure with successful incorporation of hydroxyapatite particles in composite scaffolds.

5.1.2. EDX analysis

The EDX analysis (Figure 2) of K/HA/HPMC scaffolds showed that the inorganic phase was mainly composed of calcium and phosphorous ions. The calcium to phosphorous mole ratio of composite scaffold was found to be between 1.67 and 1.73 respectively.

5.2. Physical characterization

5.2.1. X-ray diffraction

The XRD patterns to study and compare the crystalline structures of pure keratin, hydroxyapatite, HPMC and k/HA/HPMC composite scaffold are shown in Figure 3.

Figure 3(a) shows the X-ray diffraction peaks of pure keratin powder. The peaks observed at 2 Θ = 10° and 20° correspond to α-helix and β – folded structures.

The characteristic diffraction peaks for hydroxyapatite powder observed at 25.9° (002) and 31.8° (211) respectively [55].

The XRD pattern of k/HA/HPMC composite scaffolds is shown in Figure 3(d). It exhibited the diffraction peaks of both HA and keratin. Thus, the hydroxyapatite present in composite scaffold retained its crystallographic structure. It further confirms the crosslinking of hydroxyapatite with –OH and –NH_2 groups of keratin and HPMC [56].

Figure 3(b) shows the diffraction peaks of HPMC at 2Θ = 20°. These peaks were not observed in K/HA/HPMC composite scaffolds due to the possible crosslinking with HA. This decreased crystallinity of HA in K/HA/HPMC scaffolds and absence of HPMC peaks in the XRD pattern of scaffold was due to the strong crosslinking between the relevant functional groups at the organic and inorganic interface. Furthermore, the supplementary info showing wide 2 Theta range of X-ray diffraction patterns of all tested samples. The diffraction peaks of keratin powder, HPMC, hydroxyapatite powder and keratin/HA/HPMC composite scaffolds are shown in Figures S1, S2, S3 and S4 respectively.

5.2.2. Morphological and microstructural analysis using scanning electron microscopy (SEM) & microcomputed tomography (μ-CT)

The microstructure of the K/HA/HPMC scaffold was studied using SEM as shown in Figure 4(C&D). The SEM analysis of the keratin and K/HA/HPMC scaffolds showed an interconnected continuous porous structure. The average pore size observed for HPMC crosslinked keratin/HA scaffolds was 108.36 ± 22.56 μm as compared to pore size of 179 ± 36.13μm of pure keratin scaffolds respectively. Figure 4 (d) shows that the incorporation of hydroxyapatite in keratin scaffold along with HPMC

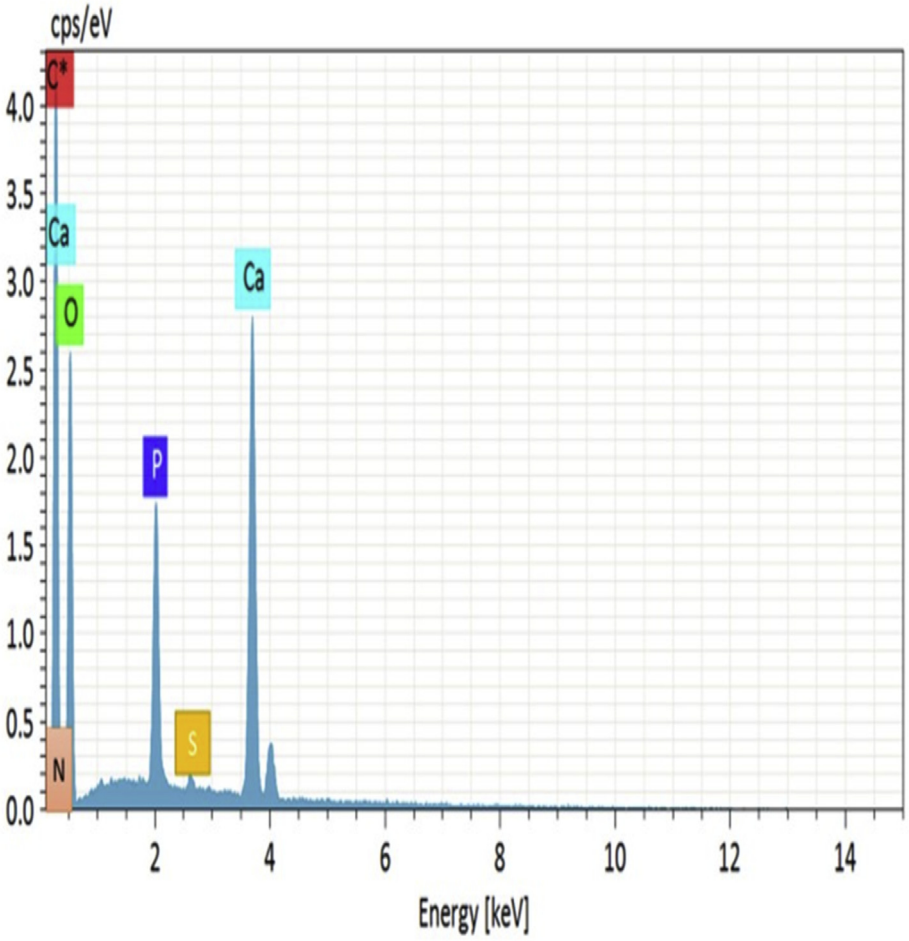

Figure 2. EDX spectra of keratin/HA/HPMC scaffold.

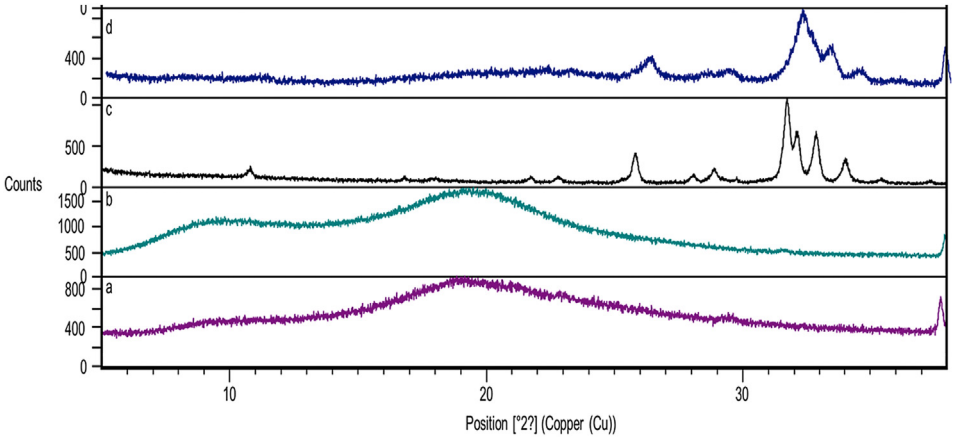

Figure 3. X-ray diffraction pattern of (a) keratin powder (b) HPMC (c) hydroxyapatite powder (d) keratin/HA/HPMC composite scaffold.

as crosslinker resulted in significant decrease in pore size. However, the reversible gelation properties of HPMC assists the formation of highly porous construct closely mimicking the spongy cancellous bone [52]. The interconnected porous network and average pore size plays an essential role during bone regeneration. According to previous studies, the average pore size in the range of 85–325um facilitate the cellular migration along with diffusion of body fluids [52, 57].

Micro-CT analysis of keratin/HA/HPMC scaffold measured the total porosity to be 79.65 %μm as shown in Figure 5. The porosity of the scaffold is an important feature from morphological perspective as it determines the degree of cellular attachment, proliferation, differentiation of osteoblasts, thus plays a crucial role in new bone formation [58]. This highly porous nature also provides additional structural stability to the implanted scaffold due to better mechanical interlocking with the surrounding bone [59]. The addition of HPMC not only provides additional sites of interaction for keratin and hydroxyapatite but also results in the formation of highly porous anisotropic structure which closely emulate the architecture of trabecular bone.

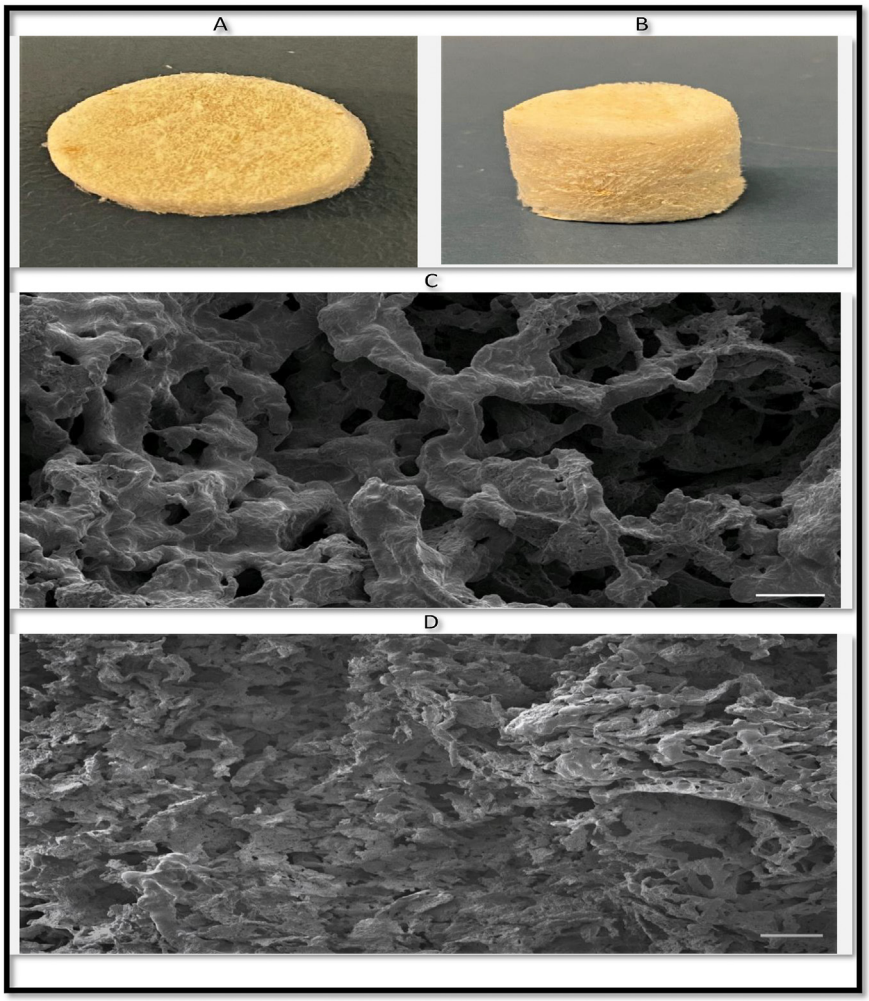

Figure 4. General Appearance of Keratin/HA/HMPMC scaffolds (diameter: 15 mm, height: 5 mm) (A & B), SEM micrographs of Pure keratin scaffolds (C) and Keratin/HA/MPMC scaffolds (D). (Size bars in figure 4 C & D represents 100 μm).

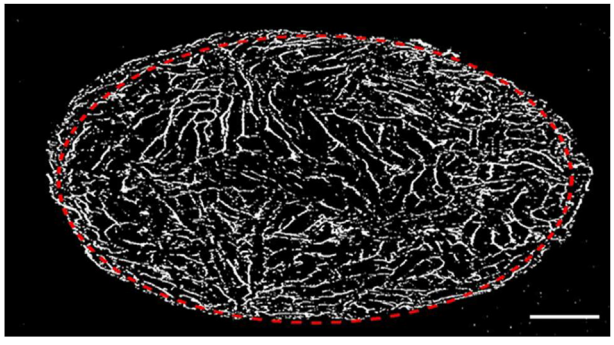

Figure 5. 2-D μ-CT image of porous keratin/HA/HPMC scaffold. Bar = 2mm.

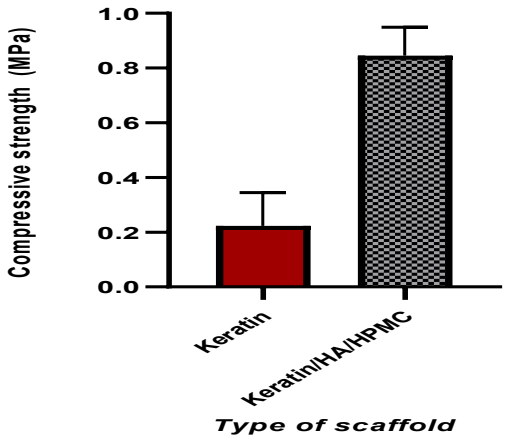

Figure 6. Graphical representation of compressive strength of pure keratin and keratin/HA/HPMC (n = 10, t-test, ****P < 0.0001).

5.3. Evaluation of mechanical properties

The mechanical property of the prepared scaffold mainly influenced by its composition, pore sizes and porosity [52]. It is an important factor in determining the applicability of the construct which has undergone above investigations, for bone regeneration. The compressive strength measurement of pure keratin sponges measured was 0.223 ± 0.12 MPa. The incorporation of HPMC and hydroxyapatite resulted in improved compressive strength of K/HA/HPMC scaffolds as shown in Figure 6.

The mean compressive strength of K/HA/HPMC scaffolds was 0.845 ± 0.10 MPa. The scaffold plays a critical role in providing initial mechanical support for the formation of new bone at the implant site. For successful clinical application, the bone repairing scaffold should possess

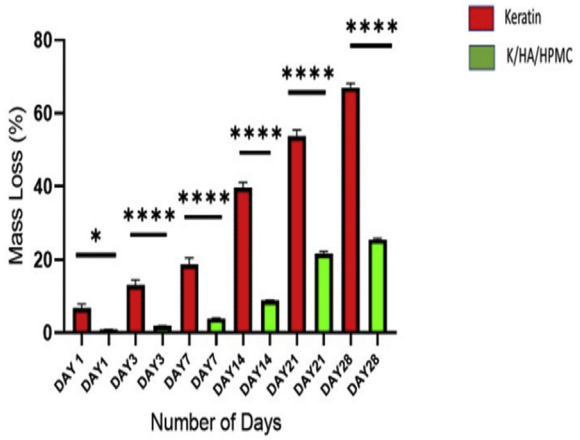

Figure 7. In vitro biodegradation of pure keratin and keratin/HA/HPMC scaffolds: average weight loss by scaffold after 1,3,7,14,21 and 28 days of immersion in PBS (n = 3, result analysed using Anova, *$P = 0.03$, ****$P < 0.0001$, error bars present ±SE of the mean).

mechanical properties similar/close to the bone that's being replaced [60]. The compressive strength of the keratin/HA/HPMC scaffold was found to be in the range of human trabecular bone (0.70–15 MPa) which further aids in the bone regeneration if implanted for trabecular bone repair [61]. Based on literature, we can expect that the mechanical strength of keratin/HA/HPMC scaffolds further increased upon implantation. Dias et al. observed significant increase in mechanical properties of implanted porous keratin-HA scaffolds in ovine models after four weeks of implantation due to new bone ingrowth by host osteoblast cells [62]. Thus, as evident from the initial results of characterization that the hydroxyapatite particles were well distributed in the crosslinked polymeric matrix which resulted in improved compressive strength of the overall scaffold.

5.4. Biodegradation

The main limitation of keratin-based biomaterials for bone tissue engineering is their fragile nature [63]. Several efforts have been made to cross link or blend keratin with other materials to improve their mechanical properties [32]. The 3D composites prepared previously by physical blending of wool derived keratin with chitosan, wool derived keratin with hydroxyapatite, horn derived keratin with collagen and polyethylene oxide blended with wool keratin showed significant improvement in mechanical strength [39, 64, 65, 66]. However, these composites were mechanically unstable and dissolve rapidly in hydrated state. The degradation behaviour of pure keratin and keratin/HA/HPMC scaffolds were studied in detail. Figure 7 represents the in vitro degradation of the pure keratin and keratin/HA/HPMC scaffold for the observed time points. The scaffolds were placed in PBS for total of 28 days and rate of weight loss was measured at 1, 3, 7, 14, 21 and 28 days respectively. The pure keratin scaffolds showed significantly higher weight loss for each time point compared to the K/HA/HPMC scaffolds (Anova, $P < 0.0001$). After 28 days of immersion in PBS a total of ~67 % weight loss was observed for pure keratin scaffolds. These lyophilized pure keratin scaffolds were too fragile to handle and lost their compact 3 -dimensional porous structure after soaking for 28 days.

In contrast, K/HA/HPMC scaffolds showed a total weight loss of just ~26% after 28 days of immersion in PBS. Keratin is insoluble in most of organic solvent, alkali/acidic solutions and water whereas, HPMC is hydrophilic in nature [8]. However, the scaffolds retained their overall shape even after 28 days of soaking, thus confirming their structural stability. Initially, after one week, the percentage of weight loss

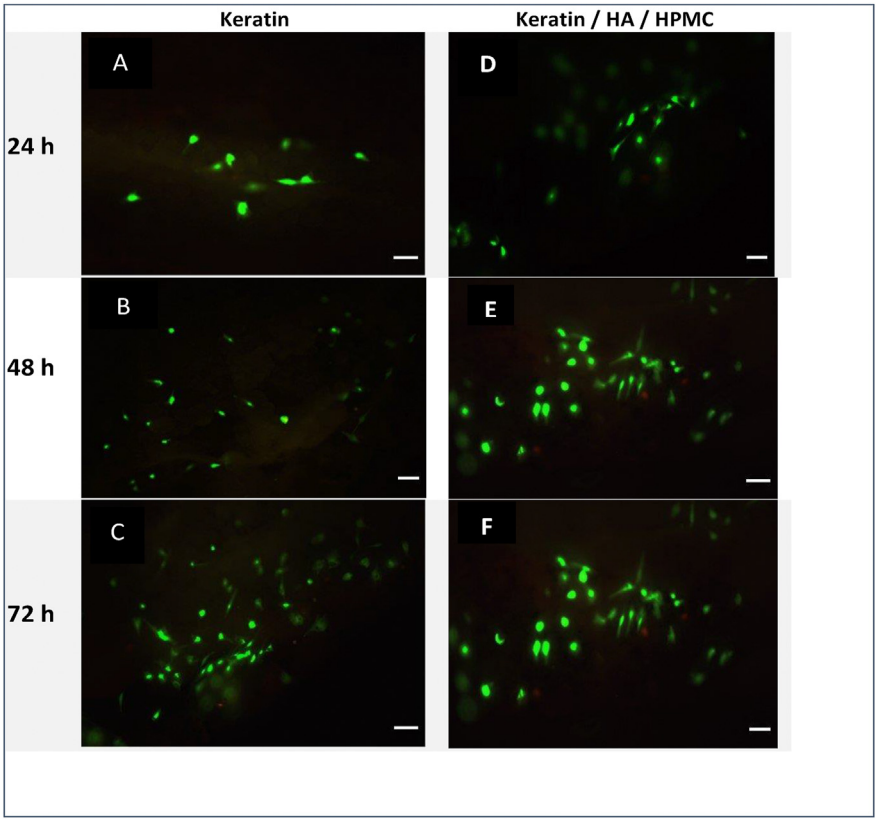

Figure 8. Fluorescence images of keratin (A, B, C) and keratin/HA/HPMC scaffolds (D, E, F) seeded with Saos-2 cells after live/dead viability assay. Images shows Saos-2 cell viability at 24 h, 48 h & 72 h. Bar = 100μm.

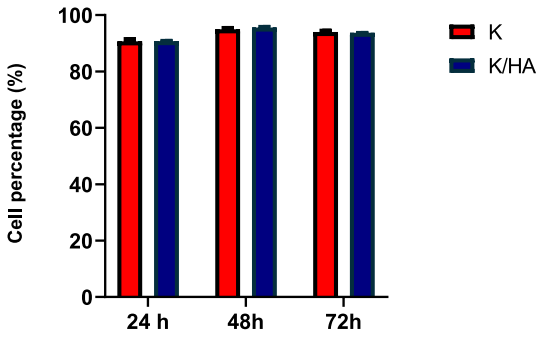

Figure 9. Saos-2 cells viability on pure keratin and keratin/HA/HPMC scaffolds at 24, 48 and 72 h (n = 3, error bars represent ±SEM).

observed was ~3.99 % and the weight loss rate increased beyond that point. Thus, the resorbability and degradation behaviour of porous keratin/HA/HPMC scaffolds showed that even at 26% weight loss at 28 days, these matrices retained their original shape while immersed in PBS.

5.5. Cytocompatibility of keratin/HA/HPMC scaffolds

Figure 8 shows confocal micrographs of keratin and keratin/HA/HPMC scaffolds seeded with Saos-2 cells at 24, 48 and 72 h respectively. Fluorescence staining was performed to observe the presence of live and dead cells. The assay solution containing 3 μl of ethidium homodimer-1 and 1.5μl of calcein AM pipetted onto each tested scaffold. After 30 min incubation at 37°C, the cell seeded scaffolds were visualized with confocal laser scanning microscope. Live cells appeared green because of the enzymatic conversion of "calcein AM" to calcein (excitation 495, emission 515nm). Dead cells emitted red fluorescence (excitation 495nm, emission 635nm) because of the binding of ethidium homodimer-1 to nucleic acids of dead cells having damaged cell membrane. The results showed excellent cell viability both for keratin and keratin/HA/HPMC scaffolds. The significant increase in cell viability was observed for all tested samples from 24 to 72 h as shown in Figure 9. However, only a slight increase in viability was observed for keratin scaffolds. It must be noted that there were no significant differences observed between keratin and keratin/HA/HPMC scaffolds at 24-, 48- and 72-hours' time point.

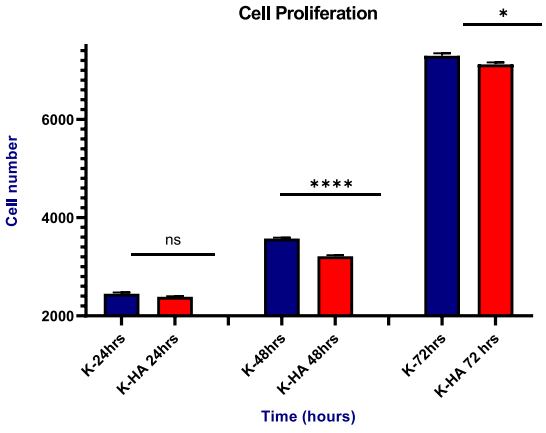

Figure 10. Saos-2 cells proliferation on keratin/HA/HPMC scaffolds at 24, 48 and 72 h. (n = 3, ****P˂0.0001, *P = 0.0240, and the error bars show the standard error of mean).

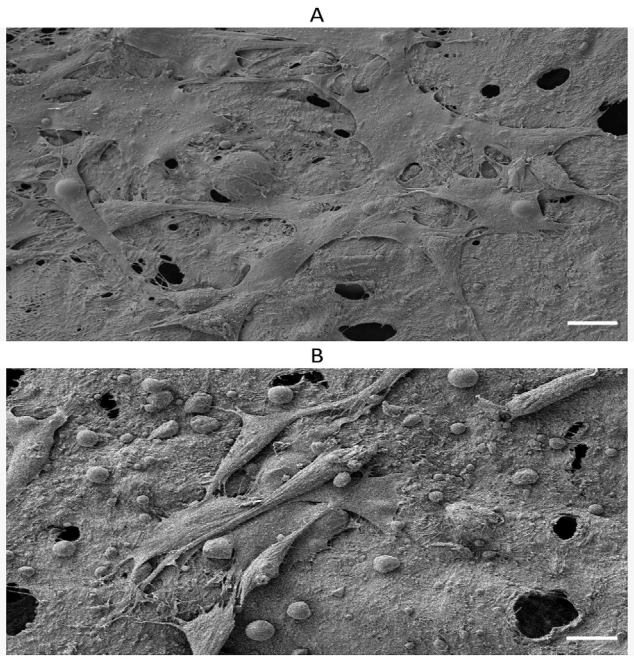

Figure 11. (A): SEM image of Saos-2 cells on scaffolds showing extracellular mesh like network (B) The intercellular connections in the form of long cytoplasmic extension which facilitates the cellular attachments with in the highly porous matrices. Scale bars in figure 11 A & B represents 10 μm.

5.5.1. Cell proliferation

MTS assay was carried out to determine the cell proliferation of keratin and keratin/HA/HPMC composite scaffold. The number of Saos-2 cells increased with incubation time in both scaffolds as shown in Figure 10. There were no significant differences in cell number between keratin and keratin/HA/HPMC at 24h time point (P = 0.7967). However, a significant increase in cell number was seen in pure keratin scaffolds compared to keratin/HA/HPMC scaffolds at 48 and 72 h (p = 0.0240), respectively. According to literature, the presence of hydroxyapatite can induce osteogenic differentiation which results in lower cellular proliferation. . Li Chen et al. also observed decreased cell density in the collagen/HA compared to pure collagen scaffolds at day 3 and 7 of culturing BMSCs [17]. Another study conducted by Eosoly et al, where increase in hydroxyapatite content in a composite, result in significantly lower cellular proliferation [67]. The cellular differentiation and osteoinductive activity of the keratin/HA/HPMC composites scaffold were not tested, which is a limitation of current study. The alkaline phosphatase activity would determine the Saos-2 cells differentiation which would promote the extracellular bone matrix formation. Therefore, the next phase of this study should be to investigate the osteoinductive properties of the keratin/HA/HPMC scaffold along with its clinical evaluation in an in vivo study as a bone graft substitute material. These results indicated that both scaffolds can promote the cellular adhesion, growth, proliferation and thus, have good biocompatibility.

5.5.2. Cell adhesion and morphology

Saos-2 cell adhesion and morphology were studied on HPMC cross-linked keratin/HA scaffolds by Scanning electron microscopy at three time points (24, 48 and 72 h). The topography of the scaffold surface plays an important role in cellular adhesion. Figure 11 shows that cells were adherent and proliferating on the porous scaffolds having 30-48um cytoplasmic extensions which appeared to be the mesh-like network of microfilaments. The surface images also showed the sheet like morphology involving surrounding cells which is the initiation of multilayer structure formation [68]. Thus, these results further signify

the fact that Saos-2 have higher affinity to attachment, proliferation and migration in HPMC crosslinked scaffolds.

6. Conclusion and future directions

A novel composite scaffold was fabricated successfully using NZ-sourced sheep wool derived keratin along with incorporation of HPMC and hydroxyapatite by using simple freeze-drying technique. The prepared scaffold showed highly porous interconnected network having pore sizes in the range of 108.36 ± 22.56 um. The maximum compressive strength was also found to be in the range of human trabecular bone which aids when implanted as a bone substitute for bone tissue regeneration. The in vitro biodegradation revealed overall 26% weight loss after 28 days in PBS immersion which confirms the structural stability of the prepared construct. Similarly, in vitro biocompatibility testing of K/HA/HPMC scaffolds seeded with osteoblast like Saos-2 cells showed high cell viability, adhesion, and affinity to proliferate across the tested scaffolds. Thus, the prepared scaffold closely mimic the trabecular part of alveolar bone and our results showed its potential application for bone tissue engineering.

However, long term in vivo studies need to be conducted in the future to further investigate the bone healing capacity of the keratin/HA/HPMC scaffold when implanted at various sites in the skeleton including the jaw alveolar bone in an animal model for bone regeneration.

Declarations

Author contribution statement

Sandleen Feroz: Conceived and designed the experiments; Performed the experiments; Analyzed and interpreted the data; Wrote the paper.

George Dias: Contributed reagents, materials, analysis tools or data.

Funding statement

This work was supported by Department of Anatomy, University of Otago.

Data availability statement

Data included in article/supplementary material/referenced in article.

Declaration of interests statement

The authors declare no conflict of interest.

Additional information

Supplementary content related to this article has been published online at https://doi.org/10.1016/j.heliyon.2021.e08294.

Acknowledgements

We would also like to thank technical assistance provided by Otago Center of Electron Microscopy (OCEM), Dr Nawshad Muhammad for this valuable input and Gemma Ker for her support with XRD testing.

References

[1] A. Cheng, C. Daly, R. Logan, B. Stein, A. Goss, Alveolar bone and the bisphosphonates, Aust. Dent. J. 54 (2009) S51–S61.
[2] D.P. Tarnow, R.N. Eskow, J. Zamzok, Aesthetics and implant dentistry, Periodontology 11 (1) (2000) 85–94, 1996.
[3] R. Gupta, K.K. Weber, Dental Implants, 2017.
[4] M.P. Sakshi, A. Yadav, P. Bajaj, K. Sharma, Knowledge and awareness of dental implants among undergraduate dental students, IP Ann. Prosthodont. Restor. Dent. 4 (2020) 6–8.
[5] L. Tolstunov, J.F.E. Hamrick, V. Broumand, D. Shilo, A. Rachmiel, Bone augmentation techniques for horizontal and vertical alveolar ridge deficiency in oral implantology, Oral Maxillofac. Surg. Clin. 31 (2) (2019) 163–191.
[6] E. Mijiritsky, Z. Mazor, A. Lorean, L. Levin, Implant diameter and length influence on survival: interim results during the first 2 years of function of implants by a single manufacturer, Implant Dent. 22 (4) (2013) 394–398.
[7] J.-H. Lee, V. Frias, K.-W. Lee, R.F. Wright, Effect of implant size and shape on implant success rates: a literature review, J. Prosthet. Dent 94 (4) (2005) 377–381.
[8] S. Feroz, N. Muhammad, J. Ranayake, G. Dias, Keratin-Based materials for biomedical applications, Bioactive Mater. 5 (3) (2020) 496–509.
[9] G. Battafarano, M. Rossi, V. De Martino, F. Marampon, L. Borro, A. Secinaro, et al., Strategies for bone regeneration: from graft to tissue engineering, Int. J. Mol. Sci. 22 (3) (2021) 1128.
[10] S. Feroz, A.S. Khan, Fluoride-substituted hydroxyapatite. Handbook of Ionic Substituted Hydroxyapatites, Elsevier, 2020, pp. 175–196.
[11] S. Feroz, F. Moeen, S.N. Haq, Protective effect of chicken egg shell powder solution (CESP) on artificially induced dental erosion: an in vitro atomic force microscope study, Int. J. Dent. Sci. Res. 5 (3) (2017) 49–55.
[12] X. Zhao, H. Xu, G. Ye, C. Li, L. Wang, F. Hu, et al., Temperature-activated PRP–cryogel for long-term osteogenesis of adipose-derived stem cells to promote bone repair, Mater. Chem. Front. 5 (1) (2021) 396–405.
[13] L. Nie, D. Chen, J. Suo, P. Zou, S. Feng, Q. Yang, et al., Physicochemical characterization and biocompatibility in vitro of biphasic calcium phosphate/polyvinyl alcohol scaffolds prepared by freeze-drying method for bone tissue engineering applications, Colloids Surf. B Biointerfaces 100 (2012) 169–176.
[14] A.A. Al-Munajjed, N.A. Plunkett, J.P. Gleeson, T. Weber, C. Jungreuthmayer, T. Levingstone, et al., Development of a biomimetic collagen-hydroxyapatite scaffold for bone tissue engineering using a SBF immersion technique, J. Biomed. Mater. Res. Part B 90 (2) (2009) 584–591. Applied Biomaterials: An Official Journal of The Society for Biomaterials, The Japanese Society for Biomaterials, and The Australian Society for Biomaterials and the Korean Society for Biomaterials.
[15] S. Rethinam, A.W. Aruni, S. Vijayan, C. Munusamy, N. Gobi, Enhanced bone regeneration using an electrospun nanofibrous membrane–a novel approach, J. Drug Deliv. Sci. Technol. 53 (2019) 101163.
[16] R.A. Surmenev, S. Shkarina, D.S. Syromotina, E.V. Melnik, R. Shkarin, Selezneva II, et al., Characterization of biomimetic silicate-and strontium-containing hydroxyapatite microparticles embedded in biodegradable electrospun polycaprolactone scaffolds for bone regeneration, Eur. Polym. J. 113 (2019) 67–77.
[17] L. Chen, Z. Wu, Y. Zhou, L. Li, Y. Wang, Z. Wang, et al., Biomimetic porous collagen/hydroxyapatite scaffold for bone tissue engineering, J. Appl. Polym. Sci. 134 (37) (2017) 45271.
[18] J. Fan, M.-Y. Yu, Y.-H. Wang, F.-Y. Cao, X. Qin, Y. Liu, In vivo biocompatibility and improved compression strength of reinforced keratin/hydroxyapatite scaffold, Tissue Eng. Regen. Med. 15 (2) (2018) 145–154.
[19] Z. Fereshteh, Freeze-drying technologies for 3D scaffold engineering. Functional 3D Tissue Engineering Scaffolds, Elsevier, 2018, pp. 151–174.
[20] W.Y. Yeong, C.K. Chua, K.F. Leong, M. Chandrasekaran, M.W. Lee, Comparison of drying methods in the fabrication of collagen scaffold via indirect rapid prototyping, J. Biomed. Mater. Res. B Appl. Biomater. 82 (1) (2007) 260–266.
[21] A.R. do Vale Morais, É. do Nascimento Alencar, F.H.X. Júnior, C.M. De Oliveira, H.R. Marcelino, G. Barratt, et al., Freeze-drying of emulsified systems: a review, Int. J. Pharm. 503 (1-2) (2016) 102–114.
[22] S. Wu, X. Liu, K.W. Yeung, C. Liu, X. Yang, Biomimetic porous scaffolds for bone tissue engineering, Mater. Sci. Eng. R Rep. 80 (2014) 1–36.
[23] J. Yan, T. Wu, Z. Ding, X. Li, Preparation and characterization of carbon nanotubes/chitosan composite foam with enhanced elastic property, Carbohydr. Polym. 136 (2016) 1288–1296.
[24] X. Wu, Y. Liu, X. Li, P. Wen, Y. Zhang, Y. Long, et al., Preparation of aligned porous gelatin scaffolds by unidirectional freeze-drying method, Acta Biomater. 6 (3) (2010) 1167–1177.
[25] S. Khorshidi, A. Solouk, H. Mirzadeh, S. Mazinani, J.M. Lagaron, S. Sharifi, et al., A review of key challenges of electrospun scaffolds for tissue-engineering applications, J. Tissue Eng. Regen. Med. 10 (9) (2016) 715–738.
[26] K. Luetzow, F. Klein, T. Weigel, R. Apostel, A. Weiss, A. Lendlein, Formation of poly (ε-caprolactone) scaffolds loaded with small molecules by integrated processes, J. Biomech. 40 (2007) S80–S88.
[27] M. Alizadeh, F. Abbasi, A. Khoshfetrat, H. Ghaleh, Microstructure and characteristic properties of gelatin/chitosan scaffold prepared by a combined freeze-drying/leaching method, Mater. Sci. Eng. C 33 (7) (2013) 3958–3967.
[28] S. Chen, T. Nakamoto, N. Kawazoe, G. Chen, Engineering multi-layered skeletal muscle tissue by using 3D microgrooved collagen scaffolds, Biomaterials 73 (2015) 23–31.
[29] N. Monmaturapoj, W. Soodsawang, W. Thepsuwan, Porous hydroxyapatite scaffolds produced by the combination of the gel-casting and freeze drying techniques, J. Porous Mater. 19 (4) (2012) 441–447.
[30] J. Wu, S. Liu, L. He, H. Wang, C. He, C. Fan, et al., Electrospun nanoyarn scaffold and its application in tissue engineering, Mater. Lett. 89 (2012) 146–149.
[31] C. Vaquette, J. Cooper-White, A simple method for fabricating 3-D multilayered composite scaffolds, Acta Biomater. 9 (1) (2013) 4599–4608.
[32] S. Feroz, N. Muhammad, J. Ratnayake, G. Dias, Keratin-Based materials for biomedical applications, Bioactive Mater. 5 (3) (2020) 496–509.

[33] C.R. Chilakamarry, S. Mahmood, S.N.B.M. Saffe, M.A.B. Arifin, A. Gupta, M.Y. Sikkandar, et al., Extraction and application of keratin from natural resources: a review, 3 Biotech 11 (5) (2021) 1–12.
[34] S.C. Cox, J.A. Thornby, G.J. Gibbons, M.A. Williams, K.K. Mallick, 3D printing of porous hydroxyapatite scaffolds intended for use in bone tissue engineering applications, Mater. Sci. Eng. C 47 (2015) 237–247.
[35] D. Tadic, F. Beckmann, K. Schwarz, M. Epple, A novel method to produce hydroxyapatite objects with interconnecting porosity that avoids sintering, Biomaterials 25 (16) (2004) 3335–3340.
[36] A. Lovati, S. Lopa, C. Recordati, G. Talo, C. Turrisi, M. Bottagisio, et al., In vivo bone formation within engineered hydroxyapatite scaffolds in a sheep model, Calcif. Tissue Int. 99 (2) (2016) 209–223.
[37] T.A. Levingstone, Matsiko, G.R. Dickson, F.J. O'Brien, J.P. Gleeson, Acta Biomater 10, 2014, p. 1996.
[38] G.J. Dias, P. Mahoney, M. Swain, R.J. Kelly, R.A. Smith, M.A. Ali, Keratin–hydroxyapatite composites: biocompatibility, osseointegration, and physical properties in an ovine model, J. Biomed. Mater. Res. 95 (4) (2010) 1084–1095.
[39] A. Tachibana, S. Kaneko, T. Tanabe, K. Yamauchi, Rapid fabrication of keratin–hydroxyapatite hybrid sponges toward osteoblast cultivation and differentiation, Biomaterials 26 (3) (2005) 297–302.
[40] G.J. Dias, P. Mahoney, N.A. Hung, L.A. Sharma, P. Kalita, R.A. Smith, et al., Osteoconduction in keratin–hydroxyapatite composite bone-graft substitutes, J. Biomed. Mater. Res. B Appl. Biomater. 105 (7) (2017) 2034–2044.
[41] G. Thakur, F.C. Rodrigues, K. Singh, Crosslinking biopolymers for advanced drug delivery and tissue engineering applications, Cutting-Edge Enab. Technol. Regener. Med. (2018) 213–231.
[42] A. Oryan, A. Kamali, A. Moshiri, H. Baharvand, H. Daemi, Chemical crosslinking of biopolymeric scaffolds: current knowledge and future directions of crosslinked engineered bone scaffolds, Int. J. Biol. Macromol. 107 (2018) 678–688.
[43] J.G. Rouse, M.E. Van Dyke, A review of keratin-based biomaterials for biomedical applications, Materials 3 (2) (2010) 999–1014.
[44] D.J. Choi, Y. Kho, S.J. Park, Y.-J. Kim, S. Chung, C.-H. Kim, Effect of cross-linking on the dimensional stability and biocompatibility of a tailored 3D-bioprinted gelatin scaffold, Int. J. Biol. Macromol. 135 (2019) 659–667.
[45] J.W. Kim, M.J. Kim, C.S. Ki, H.J. Kim, Y.H. Park, Fabrication of bi-layer scaffold of keratin nanofiber and gelatin-methacrylate hydrogel: implications for skin graft, Int. J. Biol. Macromol. 105 (2017) 541–548.
[46] S.-S. Kim, S.-H. Lim, S.W. Cho, S.-J. Gwak, Y.-S. Hong, B.C. Chang, et al., Tissue engineering of heart valves by recellularization of glutaraldehyde-fixed porcine valves using bone marrow-derived cells, Exp. Mol. Med. 38 (3) (2006) 273–283.
[47] S.N.G.P.J. Dias, A.E.-D.A. Bekhit, L. Selvanesan, H.S. Bernhardt, Treatment of Keratin-Containing Biological Materials, Google Patents, 2019.
[48] R. Zeeshan, Z. Mutahir, H. Iqbal, M. Ali, F. Iqbal, K. Ijaz, et al., Hydroxypropylmethyl cellulose (HPMC) crosslinked chitosan (CH) based scaffolds containing bioactive glass (BG) and zinc oxide (ZnO) for alveolar bone repair, Carbohydr. Polym. 193 (2018) 9–18.
[49] R.M. Urban, T.M. Turner, D.J. Hall, S.I. Infanger, N. Cheema, T.-H. Lim, et al., An Injectable Calcium Sulfate-Based Bone Graft Putty Using Hydroxypropylmethylcellulose as the Plasticizer, SLACK Incorporated Thorofare, NJ, 2004.
[50] M. Virto, P. Frutos, S. Torrado, G. Frutos, Gentamicin release from modified acrylic bone cements with lactose and hydroxypropylmethylcellulose, Biomaterials 24 (1) (2003) 79–87.
[51] J. Zhang, W. Liu, O. Gauthier, S. Sourice, P. Pilet, G. Réthoré, et al., A simple and effective approach to prepare injectable macroporous calcium phosphate cement for bone repair: syringe-foaming using a viscous hydrophilic polymeric solution, Acta Biomater. 31 (2016) 326–338.
[52] A.F. Khan, A. Afzal, A.A. Chaudhary, M. Saleem, L. Shahzadi, A. Jamal, et al., (Hydroxypropyl) methylcellulose mediated synthesis of highly porous composite scaffolds for trabecular bone repair applications, Sci. Adv. Mater. 7 (6) (2015) 1177–1186.
[53] R. Li, D. Wang, Preparation of regenerated wool keratin films from wool keratin–ionic liquid solutions, J. Appl. Polym. Sci. 127 (4) (2013) 2648–2653.
[54] M. Jackson, H. Mantsch, Ex vivo tissue analysis by infrared spectroscopy, Encyclo. Anal. Chem. 1 (2000) 131–156.
[55] F. Mohandes, M. Salavati-Niasari, M. Fathi, Z. Fereshteh, Hydroxyapatite nanocrystals: simple preparation, characterization and formation mechanism, Mater. Sci. Eng. C 45 (2014) 29–36.
[56] L. Wang, W. Dong, Y. Xu, Synthesis and characterization of hydroxypropyl methylcellulose and ethyl acrylate graft copolymers, Carbohydr. Polym. 68 (4) (2007) 626–636.
[57] Q.L. Loh, C. Choong, Three-dimensional scaffolds for tissue engineering applications: role of porosity and pore size, Tissue Eng. B Rev. 19 (6) (2013) 485–502.
[58] Y. Kuboki, H. Takita, D. Kobayashi, E. Tsuruga, M. Inoue, M. Murata, et al., BMP-induced osteogenesis on the surface of hydroxyapatite with geometrically feasible and nonfeasible structures: topology of osteogenesis, J. Biomed. Mater. Res. 39 (2) (1998) 190–199. An Official Journal of The Society for Biomaterials, The Japanese Society for Biomaterials, and the Australian Society for Biomaterials.
[59] V. Karageorgiou, D. Kaplan, Porosity of 3D biomaterial scaffolds and osteogenesis, Biomaterials 26 (27) (2005) 5474–5491.
[60] R.C. Thomson, M.J. Yaszemski, J.M. Powers, A.G. Mikos, Fabrication of biodegradable polymer scaffolds to engineer trabecular bone, J. Biomater. Sci. Polym. Ed. 7 (1) (1996) 23–38.
[61] J.R. Woodard, A.J. Hilldore, S.K. Lan, C. Park, A.W. Morgan, J.A.C. Eurell, et al., The mechanical properties and osteoconductivity of hydroxyapatite bone scaffolds with multi-scale porosity, Biomaterials 28 (1) (2007) 45–54.
[62] G.J. Dias, P.V. Peplow, A. McLaughlin, F. Teixeira, R.J. Kelly, Biocompatibility and osseointegration of reconstituted keratin in an ovine model, J. Biomed. Mater. Res. Part A 92 (2) (2010) 513–520. An Official Journal of The Society for Biomaterials, The Japanese Society for Biomaterials, and The Australian Society for Biomaterials and the Korean Society for Biomaterials.
[63] P. Hartrianti, L.T. Nguyen, J. Johanes, S.M. Chou, P. Zhu, N.S. Tan, et al., Fabrication and characterization of a novel crosslinked human keratin-alginate sponge, J. Tissue Eng. Regen. Med. 11 (9) (2017) 2590–2602.
[64] T. Tanabe, N. Okitsu, A. Tachibana, K. Yamauchi, Preparation and characterization of keratin–chitosan composite film, Biomaterials 23 (3) (2002) 817–825.
[65] S. Balaji, R. Kumar, R. Sripriya, U. Rao, A. Mandal, P. Kakkar, et al., Characterization of keratin–collagen 3D scaffold for biomedical applications, Polym. Adv. Technol. 23 (3) (2012) 500–507.
[66] A. Aluigi, C. Vineis, A. Varesano, G. Mazzuchetti, F. Ferrero, C. Tonin, Structure and properties of keratin/PEO blend nanofibres, Eur. Polym. J. 44 (8) (2008) 2465–2475.
[67] S. Eosoly, N.E. Vrana, S. Lohfeld, M. Hindie, L. Looney, Interaction of cell culture with composition effects on the mechanical properties of polycaprolactone-hydroxyapatite scaffolds fabricated via selective laser sintering (SLS), Mater. Sci. Eng. C 32 (8) (2012) 2250–2257.
[68] H.H. Xu, C.G. Simon, Fast setting calcium phosphate–chitosan scaffold: mechanical properties and biocompatibility, Biomaterials 26 (12) (2005) 1337–1348.